J Mater Sci (2007) 42:1551–1560
DOI 10.1007/s10853-006-0819-8

Ultrafine pure aluminium through back pressure equal channel angular consolidation (BP-ECAC) of particles

K. Xia · X. Wu · T. Honma · S. P. Ringer

Received: 2 June 2006 / Accepted: 18 August 2006 / Published online: 4 January 2007

Abstract Pure Al particles were synthesised into bulk materials using back pressure equal channel angular consolidation (BP-ECAC) and further deformed up to 4 passes of ECAP at 100 °C with the application of 50 MPa in back pressure. Ingot metallurgy (IM) Al was processed under the same conditions to provide comparison. The microstructures were characterised using TEM for grain size and shape as well as misorientations. In general, the grains were finer and misorientations larger in the PM (powder metallurgy) materials than in the IM materials. The tensile strength of the PM materials was significantly higher than that of the IM materials. Different work hardening behaviours were observed between the materials after 1 pass and those after 4 passes.

K. Xia (✉) · X. Wu
Department of Mechanical and Manufacturing Engineering and ARC Centre of Excellence for Design in Light Metals, University of Melbourne, Parkville, VIC 3010, Australia
e-mail: k.xia@unimelb.edu.au

T. Honma
Australian Key Centre for Microscopy & Microanalysis, University of Sydney, Sydney, NSW 2006, Australia

S. P. Ringer
Australian Key Centre for Microscopy & Microanalysis and ARC Centre of Excellence for Design in Light Metals, University of Sydney, Sydney, NSW 2006, Australia

Introduction

Ultrafine and nanostructured materials have attracted enormous attention for their potential mechanical properties which are expected to be significantly enhanced compared to their micro-structured counterparts [1]. Bulk nanostructured materials may be built up using nanoparticles [2] or obtained from refining coarse structured materials by such processes as severe plastic deformation (SPD) [3]. One of the most effective methods of refining grain sizes through SPD is equal channel angular pressing (ECAP) [4]. It has been successfully employed to produce bulk materials with sub-micrometre grains in a wide range of alloys including those based on Al [5], Cu [6], Mg [7], Fe [8], Ni [9], and Ti [10].

In addition to grain refinement, ECAP were used to consolidate particles of various alloys into bulk materials [11–13]. Recently, back pressure equal channel angular consolidation (BP-ECAC), in which a constant back pressure is applied in the exit channel, was successfully used to improve the efficiency and quality of the consolidated material [14, 15]. Producing bulk material from particles is important because many desirable off-equilibrium structures such as supersaturated solid solution, nanostructures and amorphous phases can be more readily produced in the form of particles by non-equilibrium processing including rapid solidification and mechanical milling [16]. It is, however, critical to preserve these non-equilibrium microstructures during subsequent consolidation [17]. Processes such as BP-ECAC provide advantages over conventional sintering based ones in that much lower temperatures and shorter times are involved so that the non-equilibrium features would not be destroyed.

BP-ECAC as an effective process for consolidating micro- and nano-scaled Al particles into fully dense bulk material has been demonstrated [14, 18]. It was also found that the material consolidated from particles displayed much higher strength. It suggested that the microstructure obtained in the consolidated Al and that in the material from ECAP of ingot Al were different. In the present investigation, the microstructures and tensile properties of consolidated Al materials after up to 4 passes of ECAP were compared to those produced from ECAP of ingot Al with a view to revealing the differences between the two types of materials and exploring the potential of producing ultrafine grained materials from particles.

Experimental materials and procedures

The pure Al particles were supplied by ECKA Granules Australia. They were atomised with the following specified composition: Al > 99.7 wt%, Si < 0.10 wt%, and Fe < 0.20 wt%. The as-received particles were analysed using inductively-coupled plasma atomic emission spectroscopy which revealed the following composition: Al-0.02 wt% Si-0.11 wt% Fe, consistent with the specification. Also, analysis using a LECO RO-416DR instrument showed a relatively high oxygen content of 0.38 wt%, as expected from the presence of surface oxide layers. The cumulative volume percent of particle sizes determined using a Coulter LS130 laser analyser is shown in Fig. 1, with a 50 percentile size of ~30 μm and a maximum size of ~100 μm. The shape of the particles was irregular, as shown in Fig. 2. For comparison, a pure Al ingot with a purity of >99.9 wt% and oxygen content <0.01 wt% was also used. In the following text, a material consolidated from the Al particles will be referred to as the PM (powder metallurgy) material and one processed using Al ingot as the ingot metallurgy (IM) material.

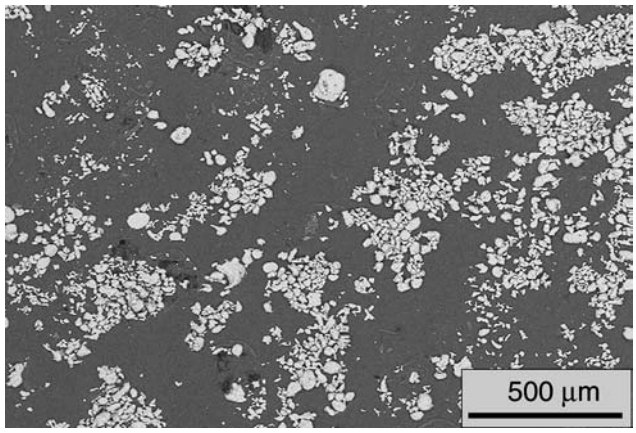

Fig. 2 SEM photo of the as-received Al particles showing irregular shape

The set-up of BP-ECAC for the PM materials (or BP-ECAP for the IM materials) consisted of a vertical entrance channel with a forward pressing plunger and a horizontal exit channel with a back plunger providing a constant back pressure during pressing, as shown in Fig. 3. The die had a 90° angle with sharp corners and channels of 9 × 9 mm in cross section. For the PM

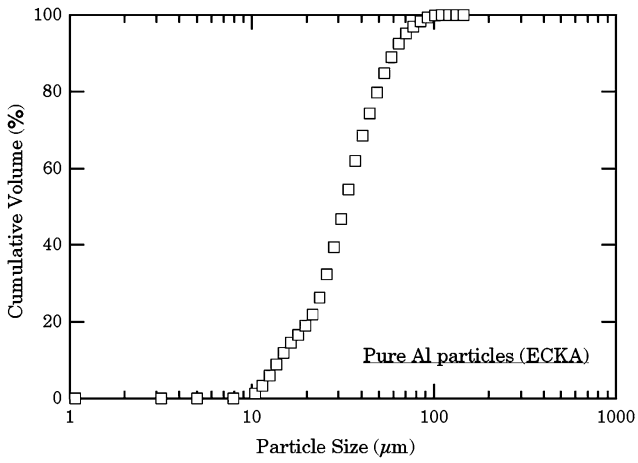

Fig. 1 Cumulative volume percent of particle sizes of the as-received Al powder

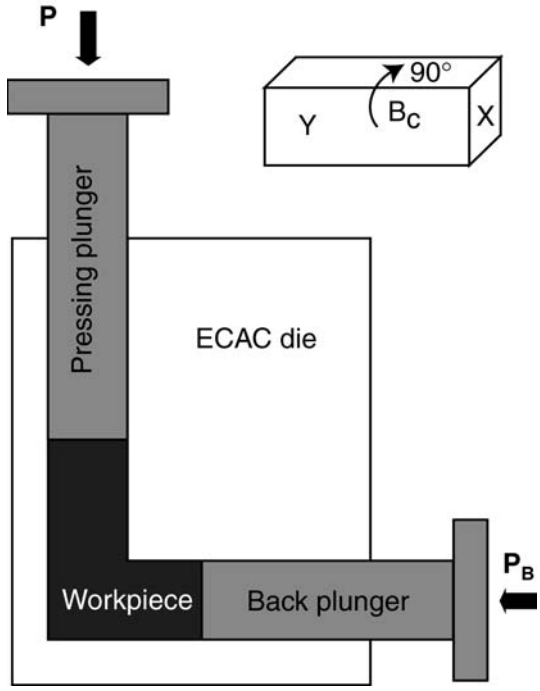

Fig. 3 The BP-ECAC/ECAP set-up

materials, the pure Al powder was wrapped in Al foil and for the IM materials, a solid Al sample was cut from the ingot. The specimen was then inserted in the entrance channel with graphite lubrication. A heating device was employed to heat the die to 100 °C which was maintained to ±1 °C through a thermal couple mounted close to the intersection of the channels. When the temperature stabilised, pressing started at a speed of 0.2 mm/min and a back pressure of 50 MPa. The specimens were ECA processed for 1 or 4 passes. The deformed sample was rotated by 90° in the same direction between passes, following the so-called B_C route, as illustrated in Fig. 3.

The microstructures of the processed materials were characterised using optical microscopy (OM), SEM and TEM. For OM and SEM, polished cross and vertical longitudinal sections (the *X* and *Y* planes in Fig. 3, respectively) were prepared following standard metallography procedures. In order to reveal the grain structures at this level, the PM materials were etched in a solution of 3 mL HF in 100 mL H_2O and the IM materials were anodised in a solution of 2.6 vol% HBF_4 in H_2O at room temperature using a voltage of 20 V for 90 s. The grain sizes were measured following ASTM standard E112-95. For TEM, slice samples were cut parallel to the cross section (i.e. the *X* plane) and mechanically polished. For the PM materials, the final thinning was done by ion milling at an angle of 13° with a voltage of 4.5 kV and current of 1 mA using a Gatan 600 DuoMill^{TM} equipped with a liquid nitrogen cooling system. For the IM materials, the foils were prepared by electropolishing in a solution of 70% ethanol and 30% nitric acid at –30 °C using a Struers Tenupol-5 with an applied potential of 30 V. The observations were carried out using a Philips CM12 operating at 120 kV. The misorientations between grains or subgrains were obtained by selected area electron diffraction (SAED) using an aperture size of 43 μm. For each material, 10–15 SAED patterns were obtained from different areas of the specimen, covering a total of several tens of grains. The grain or subgrain sizes were measured from TEM bright field images as the tangent dimensions averaged over two readings in perpendicular directions.

Density measurements based on the Archimedes principle were conducted on samples of about 2 cm^3 in volume and polished on all surfaces. The Vickers microhardness (HV) was measured on polished surface using 50 g load and 25 s loading time and the average value over ten readings was reported. For tensile testing, specimens with a gauge section of $10 \times 3 \times 2$ mm were cut along the longitudinal direction of the ECA deformed materials. Tensile tests were conducted with an initial strain rate of 3.33×10^{-4} s^{-1} at room temperature.

Experimental results

Microstructures

The SEM microstructures of the longitudinal and cross sections of the PM material after BP-ECAC for one pass are shown in Fig. 4a and b, respectively. The Al particles were well bonded into fully dense material. On the longitudinal section, the grains were elongated measuring on average ~30 and 8 μm along the long and short directions, respectively, while on the cross section, the grains were also squashed averaging ~16 μm on the long axis and ~8 μm on the short axis. For comparison, the OM microstructures of the as-cast Al ingot and the IM material after ECA deformation

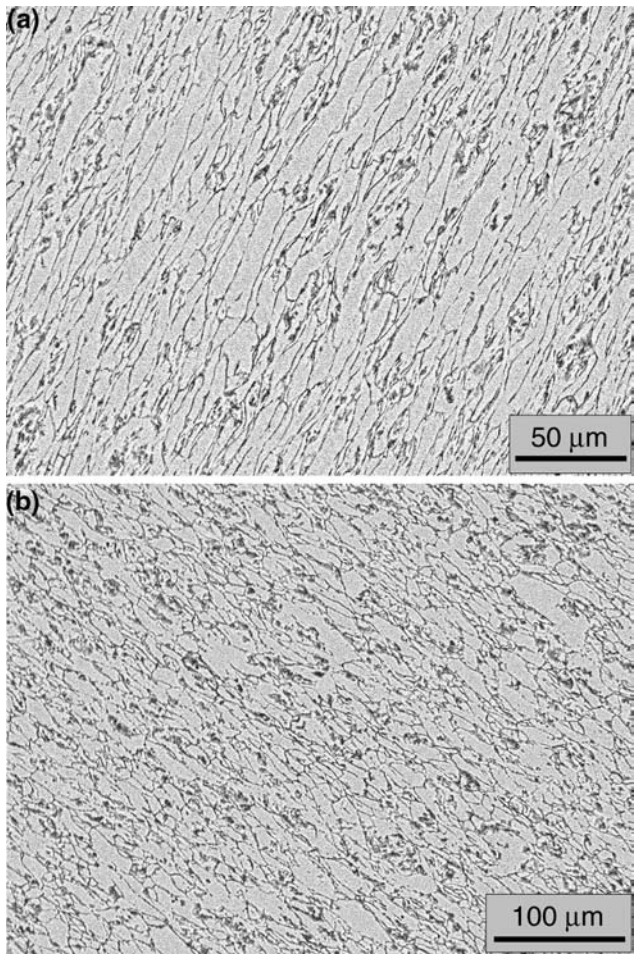

Fig. 4 SEM microstructures of the PM Al after BP-ECAC at 100 °C for one pass showing (**a**) the longitudinal section and (**b**) the cross section

for one pass are shown in Fig. 5a and b, respectively. The as-cast Al ingot was very coarse with an average grain size of ~1600 μm. The grains were refined after ECA deformation to have an average grain size of ~535 μm at the OM level of observation. The grain structures of the PM and IM materials after 4 passes were too fine to resolve using OM or SEM.

For revealing grains of the order of 1 μm or smaller in size and subgrain structures, TEM was necessary. The TEM microstructures of the PM materials after BP-ECAC for 1 and 4 passes are shown in Fig. 6a and b, respectively. The grain structure after 1 pass was obviously different from that revealed by SEM shown in Fig. 4a. The grains were not only much finer but also nearly equiaxed. The grain structure after 4 passes appeared to be similar but still finer. These observations were confirmed by the measured grain size distributions shown in Fig. 7a and b, giving rise to average grain sizes of 1058 and 828 nm for the materials after 1 and 4 passes, respectively, as listed in Table 1. In comparison, the TEM microstructures of the IM materials after BP-ECAP for 1 and 4 passes are shown in Fig. 8a and b, respectively. The grains were elongated after 1 pass similar to what was observed using OM, but much finer than revealed by OM. However, the grain structure became mostly equiaxed after 4 passes. The grain size distributions of the two materials are shown in Fig. 9a and b, and the average grain sizes were 1311 and 1265 nm, respectively.

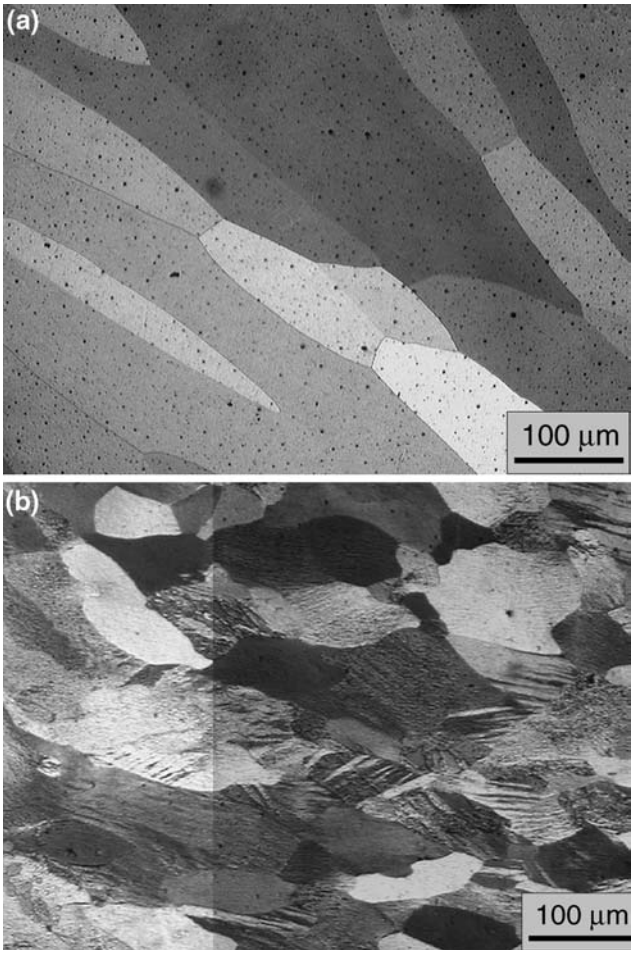

Fig. 5 OM microstructures of (**a**) the as-cast Al ingot and (**b**) the cross section of the IM material after BP-ECAP at 100 °C for 1 pass

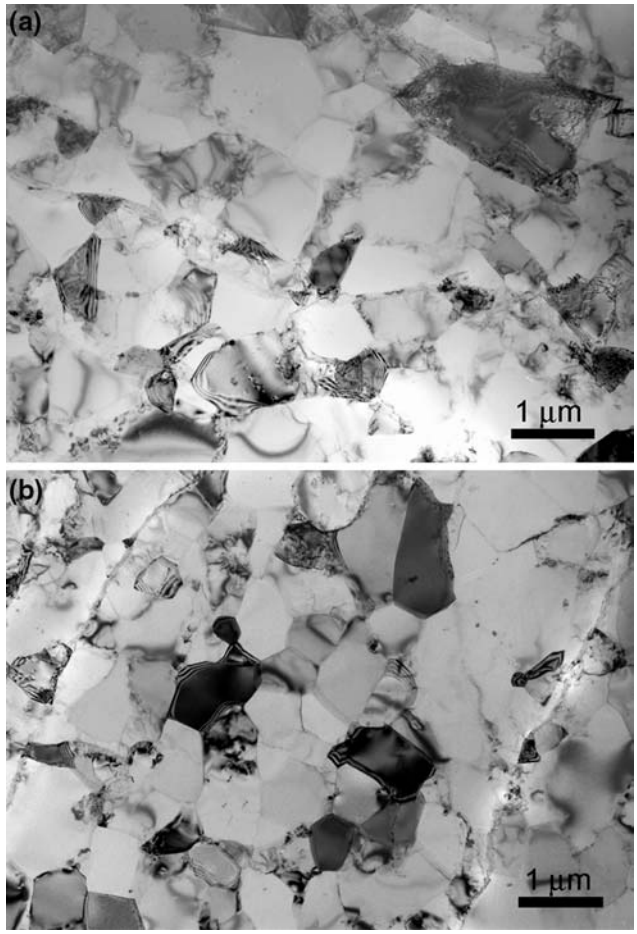

Fig. 6 TEM microstructures of the PM Al after BP-ECAC at 100 °C for (**a**) 1 pass and (**b**) 4 passes

Up to this point, the term ''grain'' has been used to refer to both grains and subgrains without distinction. To find out misorientations between grains, results from SAED were obtained and analysed. Representative SAED patterns obtained from the IM materials after 1 and 4 passes and those from the PM materials after 1 and 4 passes are shown in Fig. 10. From each pattern, the misorientation was measured, as illustrated in Fig. 10. For each material, misorientations were measured from 10 to 15 patterns obtained from different areas of the specimen. The average,

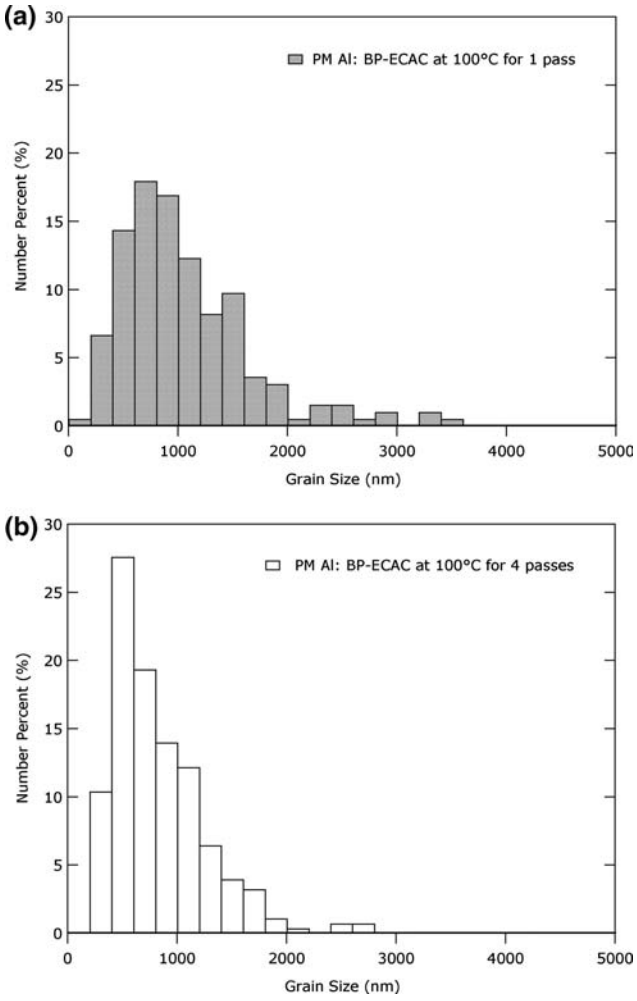

Fig. 7 Grain size distributions in the PM Al after BP-ECAC at 100 °C for (**a**) 1 pass and (**b**) 4 passes

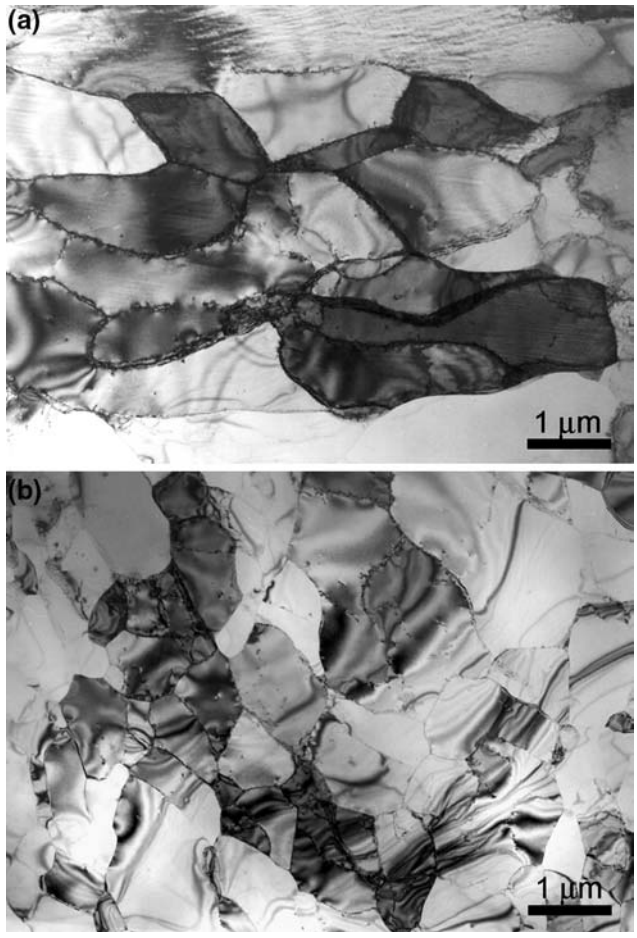

Fig. 8 TEM microstructures of the IM Al after BP-ECAP at 100 °C for (**a**) 1 pass and (**b**) 4 passes

maximum and minimum values of misorientation are plotted as a function of the number of ECAP passes in Fig. 11. The IM Al after 1 pass showed an average misorientation of ~2.6° with a maximum of ~4.9°, and thus contained mostly low angle boundaries (i.e. subgrains); after 4 passes, some large angle boundaries (maximum of ~15.1°) were developed although the average misorientation remained low at ~6.9°. In the PM Al on the other hand, a considerable number of boundaries were already large angle after 1 pass, displaying an average misorientation of ~10° and a maximum of ~20°; no significant increase in misorientation was observed after 4 passes with virtually no change in the average misorientation. In both the IM and PM Al, some small angle boundaries (<5°) remained after 4 passes, though.

Table 1 Grain/subgrain sizes of the IM and PM materials after BP-ECAP/ECAC at 100 °C for 1 and 4 passes based on TEM observations

Average grain/subgrain size (nm)	After 1 pass	After 4 passes
IM Al	1311	1265
PM Al	1058	828

Density, hardness and tensile properties

The densities of the as-cast Al ingot, the IM materials after 1 and 4 passes and the PM materials after 1 and 4 passes are listed in Table 2. The full density of pure Al (2.7 g/cm^3) was reached after the very first pass of BP-ECAC. Also presented in Table 2 are the HV values of the five materials. The cast Al ingot was significantly hardened after just one pass, as expected, and the hardness was further increased after 4 passes. In particular, the PM materials were considerably harder than the IM materials after ECAP.

The tensile stress versus strain curves for the as-cast Al ingot, the IM materials after 1 and 4 passes

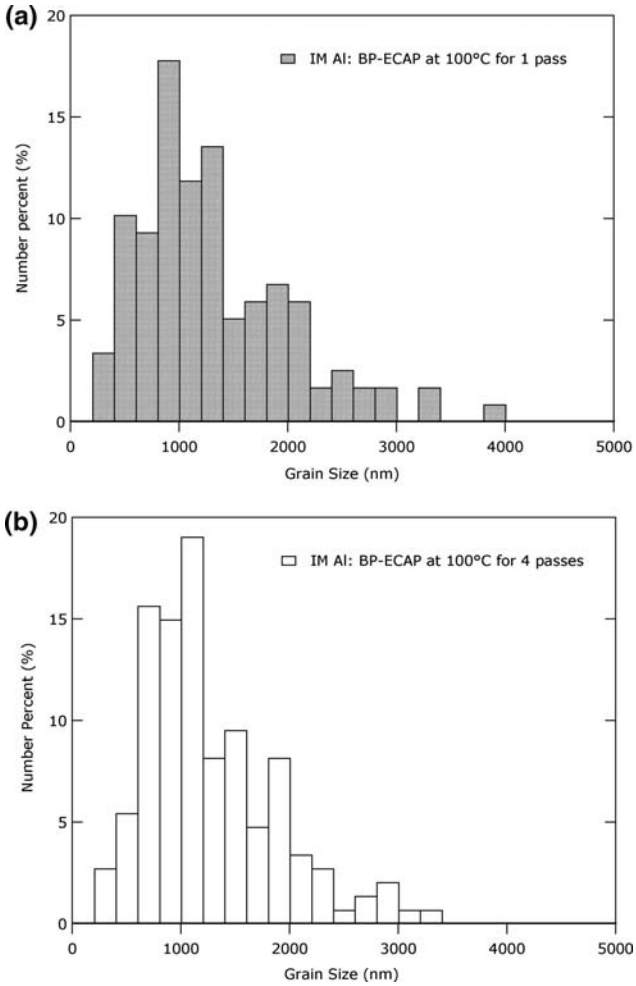

Fig. 9 Grain size distributions in the IM Al after BP-ECAP at 100 °C for (**a**) 1 pass and (**b**) 4 passes

and the PM materials after 1 and 4 passes are shown in Fig. 12. The 0.2% proof stress, ultimate tensile strength and strain to fracture are displayed in Table 2. The as-cast Al with a coarse grain structure exhibited low strength and good ductility with moderate work hardening. After 1 pass of ECAP, the yield strength was doubled whereas the ductility was significantly reduced. However, little work hardening was observed. The yield strength was further increased by 60–70% after 4 passes without any loss in ductility, although the UTS was achieved very early after yielding. On the other hand, the PM materials were significantly stronger (by about 125% after 1 pass and 72% after 4 passes) although the ductility was halved, compared to the IM materials. The absolute increase in yield strength from 1 to 4 passes was comparable to that in IM materials with, again, no loss in total elongation. Similar to the IM material, instability started early after 4 passes.

Discussion

As described in an earlier investigation [14], BP-ECAC is an effective process for consolidating particles into fully dense bulk material at low temperatures. The consolidated Al was further deformed by ECAP to 4 passes in this study, and a solid Al ingot was ECA deformed for 1 and 4 passes under the same back pressure to provide comparison. In the following discussion, the microstructures and tensile properties obtained for the IM and PM materials will be analysed and compared to those observed in IM Al undergone ECAP without back pressure with a view to revealing the deformation behaviour during ECAP under different conditions.

Microstructures after ECAP with back pressure

Despite the application of a back pressure, the TEM microstructure of the IM Al after ECAP at 100 °C for 1 pass is similar to that observed by others in IM Al after ECAP without back pressure [19–21], consisting of elongated subgrains with small angle boundaries (defined as <~10°) and an average size of ~1–1.5 μm, as shown in Figs. 8a, 10 and Table 1, although the bands of subgrains were not as well defined. (The smaller average subgrain size of ~0.6 μm in [5] was actually the average along the short direction of the subgrain bands.) After 4 passes, the subgrains became mostly equiaxed, again resembling those observed in other IM Al after multiple passes without back pressure. However, Fig. 11 indicates that the boundaries were still dominated by low angle ones although some larger angle boundaries had occurred and the average misorientation had been increased, whereas the misorientation angle had increased to >20° after the second pass without back pressure [5]. It should be noted that BP-ECAP in the present study was conducted at an elevated temperature of 100 °C and a slower pressing speed of 0.2 mm/min. Investigations by others showed no significant influence from temperature up to 100 °C [22] and pressing speed as low as 0.5 mm/min [23]. However, the subgrain structure remained after 6 passes at higher temperatures of 200 and 300 °C [22]. Since the transformation from low angle to high angle boundaries is believed to be accomplished by dislocations entering the boundary wall, this seemed to suggest that back pressure had hindered this process probably by promoting dislocation annihilation inside the subgrains. The average grain size, however, remained at ~1.3 μm, comparable to that reported in [5] (the two measurements were more comparable now that the grains were equiaxed).

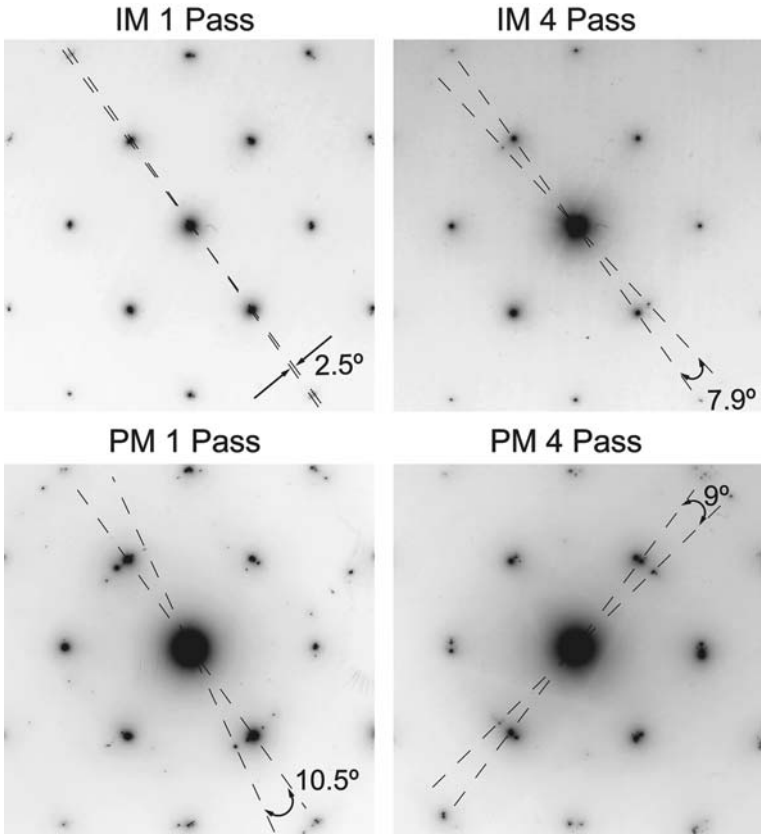

Fig. 10 Selected SAED patterns from the IM Al and PM Al after BP-ECAP at 100 °C for 1 pass and 4 passes (B//⟨110⟩)

For the PM Al, in the first pass of BP-ECAC, individual particles were sheared, as in ECAP of a solid material, and bonded to each other, leading to a microstructure with elongated grains at the SEM level of observation. It is reasonable to believe that the grain boundaries seen in Fig. 4 were those between bonded particles. Closer observations at the TEM level revealed a much finer grain structure within each particle, as shown in Fig. 6a, as happened to the IM Al. However, these ultrafine grains in the PM material were different in that they were equiaxed in shape and had a considerable number of large angle boundaries between them (Fig. 11). In other words, the ultrafine structure in the PM material consisted of many true grains while those in the IM material were mostly subgrains after the first pass. It was possible that these initial differences resulted from the completely different starting microstructures. The original Al ingot was comprised of very coarse grains (of the order of >1 mm) whereas the PM material was produced from loosely packed individual particles <0.1 mm in size. The much finer particle size favoured the formation of high angle boundaries as dislocations were blocked at the particle boundaries. The other factor to consider was the presence of oxide particles in the PM material due to particle surface. These oxide particles would retard the recovery process and thus promote the entering of dislocations into boundaries. This was consistent with observations in a Al–Mg–Sc alloy [22]: the low angle grain boundaries found in pure Al after 6 passes at 300 °C were replaced by high angle boundaries in the alloy, thanks to the presence of fine Sc containing intermetallic particles formed.

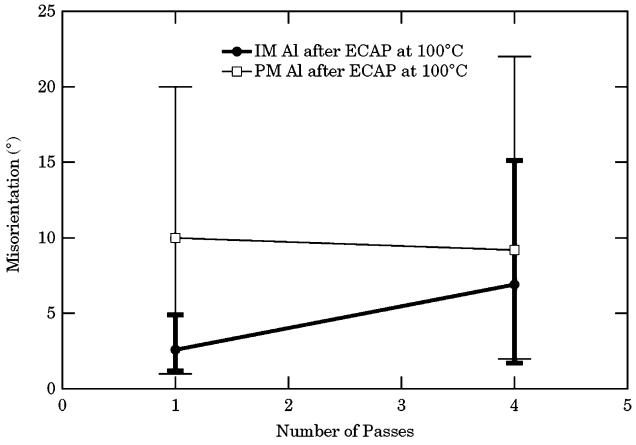

Fig. 11 Misorientation versus number of passes in the IM and PM Al after ECAP at 100 °C

The grains in the PM material after 1 pass were further refined after 4 passes, reducing the average grain size from >1000 nm to around 800 nm. The

Table 2 Density, HV and tensile properties at room temperature of the as-cast Al ingot and IM and PM Al after BP-ECAP/ECAC at 100 °C for 1 and 4 passes

Material	Density (g/cm^3)	HV (kg/mm^2)	0.2% proof stress (MPa)	UTS (MPa)	Strain to fracture (%)
As-cast Al ingot	2.70	23.5	27	41	58
IM Al after 1 pass	2.70	32.3	60	64	23
IM Al after 4 passes	2.70	38.0	99	104	25
PM Al after 1 pass	2.70	52.7	135	160	11
PM Al after 4 passes	2.70	59.1	170	179	11

average misorientation remained about the same as that after 1 pass although the maximum misorientation was slightly increased. In contrast, the grains increased slightly in size and misorientations became too large to measure in an IM Al after 4 passes without back pressure [5]. This seems to point to a possible role played by the back pressure in the evolution of the substructure more than a difference between the PM and IM materials. More careful quantitative analysis of the microstructural evolution is needed before a good understanding of the phenomenon can be gained.

Tensile properties

For convenience, the tensile characteristics for the IM and PM Al in the present investigation and those of IM Al in other studies are listed in Table 3, together with information regarding the grain size, shape and misorientation. It is readily observed from this table that PM Al was significantly stronger than the IM Al after BP-ECAP. Although the IM Al was considerably strengthened after a single pass (the yield strength was increased by 33 MPa, doubling that of the as-cast ingot), the PM material was more impressive after BP-ECAC with a yield strength more than double that of the IM counterpart (an increase of 75 MPa). This was because the PM material contained much finer grains with boundaries of higher misorientation angles, both beneficial to strength, thanks to the much finer starting Al particles and the presence of oxide particles which tended to reduce the level of recovery [26] and prevent grain growth. In addition, the oxide particles in the PM material might have contributed to the strengthening directly. However, further increases in strength after 4 passes were similar in the IM Al (by 39 MPa) and PM Al (by 35 MPa). This suggests that the evolution from 1 pass to 4 passes was similar, despite the different final microstructures which gave rise to different strengths. Although it was clear from Table 3 that strength generally increases with decreasing grain sizes, there was considerable scattering, reflecting different methods of grain size measurement and the effects of microstructural features other than the grain size. Further systematic examination of detailed microstructures is needed before any firm conclusion can be drawn.

Other significant observations can be made in Fig. 12. Despite their different strength levels (and thus different ductility), the IM and PM materials displayed very similar tensile curves after the same ECAP. That is, the flow stress reached a steady-state

Table 3 Comparison of tensile properties at room temperature of various pure Al after ECAP following the B_C route

Material	Number of passes	ECAP T (°C)	Grain size (μm) & shape	Average misorientation (°)	Yield strength (MPa)	Strain at fracture (%)	Work hardening	Reference
IM Al	1	100	1.31 elongated	2.6	60	23	Zero	Present work
PM Al	1	100	1.06 equiaxed	10	135	11	Zero	Present work
IM Al	4	100	1.27 equiaxed	6.9	99	25	Negative	Present work
PM Al	4	100	0.83 equiaxed	9.2	170	11	Negative	Present work
IM Al	1	RT	~0.6 (short axis) elongated	Low angle	~105–110	–	–	[5, 24]
IM Al	4	RT	~1.4 equiaxed	High angle	~115	–	–	[5, 24]
IM Al (ECAP plus annealing at 250 °C for 1 h)	8	RT	0.59 equiaxed	Mostly high angle	~160–170	~11	Negative	[25]

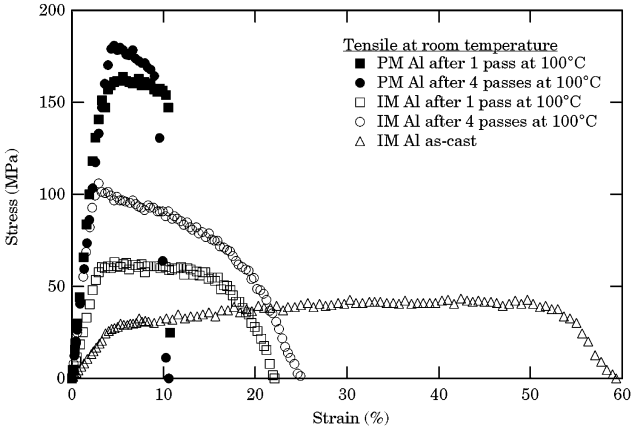

Fig. 12 Tensile curves of the as-cast, PM and IM Al after ECAC/ECAP at 100 °C for 1 pass and 4 passes

plateau shortly after yielding in the materials after 1 pass, and the flow stress started to decline almost immediately after yielding in those after 4 passes. In both cases, a substantial amount of plastic deformation was sustained despite a lack of work hardening. The decreasing flow stress after 4 passes was also observed in an IM Al following 8 passes plus annealing [25]. In another report [27], the rate of work hardening changed from positive to negative with decreasing grain sizes to below 1 μm in annealed Al after SPD. However, the results in the present study did not support the arguments that the work softening was solely due to different boundary characters [25] or ultrafine grain sizes [27]. The IM and PM materials after 1 pass in the present study had different grain sizes, shapes and boundary characters, and so did the IM and PM materials after 4 passes. The observations were also independent of strength and type of material (IM vs. PM). Therefore, the similarity in the tensile curve shapes was most apparently related to the number of passes, or the amount of plastic deformation, via the B_C route under an applied back pressure. In other words, deformation structures other than those represented by the grain size, shape and boundary misorientation angle had affected the work hardening behaviour. The steady state deformation in the Al after 1 pass reflected a dynamic balance between work hardening (mostly as a result of increase in dislocation density accompanying the tensile deformation) and work softening (due to the annihilation and rearrangement of dislocations) whereas in the Al after 4 passes, work softening was more significant. Assuming the increase in dislocation density needed to accommodate plastic deformation in the two Al was similar, it was postulated that the boundaries in the Al after 4 passes were more capable of absorbing dislocations than those after 1 pass. Careful TEM examination of the microstructures at different stages of tensile deformation in various materials is needed to clarify the issue.

Summary and conclusions

(1) Pure Al particles were ECA consolidated into fully dense materials at 100 °C under a back pressure of 50 MPa and ECA deformed further to 4 passes. For comparison, cast Al ingot was ECA deformed under the same conditions.
(2) The PM material after 1 pass consisted of ultrafine grains of ~1 μm in size and equiaxed in shape with a considerable number of high angle boundaries whereas the IM counterpart contained elongated subgrains of mostly low angle boundaries with an average size of ~1.3 μm.
(3) After 4 passes, the PM material was further refined to have equiaxed grains of ~0.8 μm with only a slight increase in the maximum misorientation. In contrast, the IM material after 4 passes showed insignificant changes in grain sizes but a moderate increase in misorientation although the grain structure had become equiaxed.
(4) The strength of the PM materials was significantly higher than that of the IM materials. The increases in yield strength from 1 pass to 4 passes, however, were similar in both materials. Correspondingly, the ductility of the PM materials was halved, compared to that of the IM materials.
(5) A steady state deformation was observed during tensile testing in the PM and IM materials after 1 pass of ECAP, while work softening occurred in both materials after 4 passes.
(6) BP-ECAC of fine particles appears to be an effective way of producing ultrafine structured materials with high strength and good ductility.

Acknowledgements This project was supported by the Australian Research Council with the ARC Centre of Excellence for Design in Light Metals and by the University of Melbourne under the Melbourne Research Grants Scheme. The supply of Al particles by ECKA Granules Australia and assistance from Comalco Research and Technical Support are gratefully acknowledged. We also acknowledge assistance received from the NANO-MNRF.

References

1. Kumar KS, Van Swygenhoven H, Suresh S (2003) Acta Mater 51:5743
2. Gleiter H (2000) Acta Mater 48:1
3. Valiev RZ, Islamgaliev RK, Alexandrov IV (2000) Prog Mater Sci 45:103

4. Langdon TG, Furukawa M, Nemoto M, Horita Z (2000) JOM 52:4–30
5. Iwahashi Y, Horita Z, Nemoto M, Langdon TG (1998) Acta Mater 46:3317
6. Dalla Torre F, Lapovok R, Sandlin J, Thomson PF, Davies CHJ, Pereloma EV (2004) Acta Mater 52:4819
7. Xia K, Wang JT, Wu X, Chen G, Gurvan M (2005) Mater Sci Eng 324:A410
8. Shin DH, Kim I, Kim J, Park K-T (2001) Acta Mater 49:1285
9. Neishi K, Horita Z, Langdon TG (2002) Mater Sci Eng A325:54
10. Stolyarov VV, Zhu YT, Alexandrov IV, Lowe TC, Valiev RZ (2003) Mater Sci Eng A343:43
11. Matsuki K, Aida T, Takeuchi T, Kusui J, Yokoe K (2000) Acta Mater 48:2625
12. Haouaoui M, Karaman I, Maier HJ, Hartwig KT (2004) Metall Mater Trans A 35A:2935
13. Senkov ON, Senkova SV, Scott JM, Miracle DB (2005) Mater Sci Eng A393:12
14. Xia K, Wu X (2005) Scr Mater 53:1225
15. Wu X, Xia K (2006) Mater Sci Forum 503–504:233
16. Suryanarayana C (1999) Non-equilibrium processing of materials. Pergamon, Oxford, UK
17. Gutmanas EY (1990) Prog Mater Sci 34:261
18. Wu X, Xia K (2006) Mater Sci Forum 519–521:1215
19. Iwahashi Y, Horita Z, Nemoto M, Langdon TG (1997) Acta Mater 45:4733
20. Chang J-Y, Yoon J-S, Kim G-H (2001) Scr Mater 45:347
21. Wu PC, Chang CP, Kao PW (2004) Mater Sci Eng A374:196
22. Yamashita A, Yamaguchi D, Horita Z, Langdon TG (2000) Mater Sci Eng A287:100
23. Berbon PB, Furukawa M, Horita Z, Nemoto M, Langdon TG (1999) Metall Mater Trans A 30A:1989
24. Furuno K, Akamatsu H, Oh-Ishi K, Furukawa M, Horita Z, Langdon TG (2004) Acta Mater 52:2497
25. Sun PL, Yu CY, Kao PW, Chang CP (2005) Scr Mater 52:265
26. Humphreys FJ, Hatherly M (1996) Recrystallization and related annealing phenomena. Pergamon, Oxford, UK, p 164
27. Tsuji N, Ito Y, Saito Y, Minamino Y (2002) Scr Mater 47:893